confirmed on the basis of HMBC spectrum, in which the same correlation as for **4** and **6** was observed. The phosphonate **21** was transformed into phosphonic acid (**22**) in 74% yield by treatment with TMSBr in CH_2Cl_2 and the resulting phosphonic acid **22** was converted into its POM ester (**8**; Piv-P-MEP-G) in 10% yield.[10)]

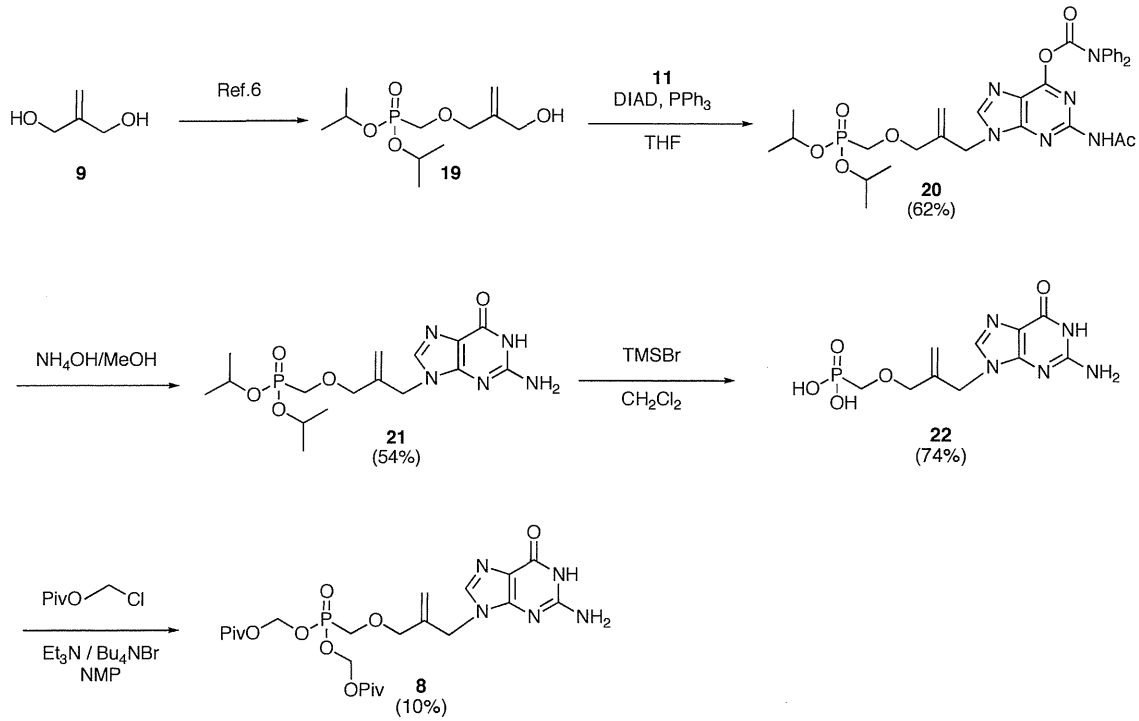

Scheme 3. Synthesis of Piv-P-MEP-G (**8**).

Biological evaluation

Evaluation of the anti-HBV activity of the novel acyclonucleosides synthesized in this study was conducted with HepG2 2.2.15 cells transfected with the HBV genome.[11)] As shown in Table 1, G-MEP **4** and G-MEB **6** did not exhibit anti-HBV activity nor

display any cytotoxicity toward HepG2 cells (entries 1 and 2). These results revealed that the conformationally-rigid cyclopentane ring of entecavir is an essential structure for antiviral activity. Moreover, inactivity of the phosphalaninates **5** and **7** suggested that the initial phosphorylation step of **4** and **6** is not responsible for the lack of the anti-HBV activity.

In contrast to the above results, the POM-protected phosphonate derivative **8** was found to possess antiviral activity with an EC_{50} of 0.29 μM. However, cytotoxicity toward HepG2 cells was also observed. With POM-protected prodrugs, it has been pointed out that the toxicity could be attributed to pivalic acid generated during the release of the parent compounds.[10b] Therefore, we have evaluated the toxicity of pivalic acid in this assay system and found that the acid did not show any cytotoxicity up to 100 μM, which most likely were ruled out this issue.

Table 1. Anti-HBV activity and cytotoxicity of **4-8**

compound	EC_{50}(μM)	CC_{50} (μM) (HepG2)
4	> 1	> 100
5	> 1	> 100
6	> 1	> 100
7	> 1	> 100
8	0.29	39

Conclusions

We have synthesized the novel exomethylene acycloguanine nucleosides MEP-G (**4**) and MEB-G (**6**). The respective monophosphate derivatives, that is, phosphoalaninate pro-drugs L-ala-P-MEP- **5** and L-ala-P-MEB-G **7** of the monophosphate of **4** and **6** were also synthesized. Furthermore, the phosphonate analog Piv-P-MEP-G (**8**) of **7** was also evaluated for anti-HBV activity. Mitsunobu-type alkylation of 2-*N*-acetyl-6-*O*-diphenylcarbamoylguanine (**11**) with the respective primary alcohols proceeded regioselectively at its N^9-position and this synthetic strategy enabled us to shorten the synthetic route for the target molecules compared to the previously reported method. Evaluation of the anti-HBV activity and its cytotoxicity toward HepG2 cells revealed that the rigidity of the aglycon moiety is an important requirement for inhibition of HBV replication. The phosphonate derivative **8** showed moderate activity with an EC_{50} of 0.29 μM and the SI was 137 although some cytotoxicity (CC_{50} of 39 μM) was observed.

Experimental Section

General

Melting points are uncorrected. Reagents and solvents were used without any further purification unless otherwise noted. Thin layer chromatography (TLC) was

performed using precoated TLC plates (Merck, Silica gel 60 F254, 0.25 mm). ^{1}H and ^{13}C NMR spectra were recorded on a JEOL ECA 500 spectrometer operating at room temperature. Chemical shifts are reported in parts per million (δ) relative to the residual solvent peak. DSS served as internal standard for ^{13}C NMR measurements in D_2O. Mass spectra analysis was performed on a JEOL JMS-T100LP.

2-Acetyl -9-[2-(*tert*-butyldimethylsilyloxymethyl)allyl]-6-*O*-diphenyl-carbamoylguanine (12)

To a solution of **10** (989 mg, 5.68 mmol), triphenylphosphine (1.49 g, 5.68 mmol) and **11** (2.10 g, 5.41mmol) in THF (50 mL) was added DIAD (1.15 g, 5.68 mmol). The reaction mixture was heated to 70 °C and stirred for 2hr. After cooling, the mixture was filtered through a celite pad. The filtrate was evaporated, and the residue was purified by silica gel column chromatography (Hexane-EtOAc 3:2 to 2:3, v/v) to provide **12** (1.71 g, 2.99 mmol, 53% yield) as a white foam. ^{1}H NMR (500 MHz, $CDCl_3$) δ 8.05 (brs, 1H), 7.95 (s, 1H), 7.43-7.25 (m, 10H), 5.23 (s, 1H), 4.96 (s, 1H), 4.80 (s, 2H), 4.10 (s, 2H), 2.56 (s, 3H), 0.89 (s, 9H), 0.05 (s, 6H); ^{13}C NMR (126 MHz, $CDCl_3$) δ 171.08, 156.09, 155.13, 152.13, 150.36, 144.18, 142.43, 141.69, 129.15, 127.08, 125.86, 120.52, 114.27, 64.08, 45.50, 25.77, 25.13, 18.22, -5.46. MS (ESI) m/z $(M+Na)^+$ calcd. 595.2465, found 595.2485.

9-[2-(*tert*-Butyldimethylsilyloxymethyl)allyl]guanine (13)

To a solution of **12** (868 mg, 1.51mmol) in methanol (6 mL) was added 28% ammonia solution (3 mL) and heated to 60 °C in sealed tube. After 2h, the reaction mixture was concentrated and purified by silica gel column chromatography (CH_2Cl_2-MeOH 92:8 to 84:16, v/v) to provide **13** (446 mg, 1.33 mmol, 88% yield) as a white solid. ^{1}H NMR (500 MHz, DMSO-d_6) δ 10.58 (brs, 1H), 7.60 (s, 1H), 6.42 (brs, 2H), 5.12 (s, 1H), 4.65 (s, 1H), 4.54 (s, 2H), 4.11 (s, 2H), 0.86 (s, 9H), 0.03 (s, 6H); ^{13}C NMR (126 MHz, DMSO-d6) δ157.05, 153.80, 151.52, 144.56, 137.67, 116.57, 110.84, 63.69, 44.20, 25.96, 18.15, -5.31; MS (ESI) m/z $(M+Na)^+$ calcd. 358.1675, found 358.1714.

9-[(Hydroxymethyl)allyl]guanine (4)

To a suspension of **13** (421 mg, 1.26 mmol) in THF (15 mL) was added 1M TBAF in THF solution (3.14 mL, 3.14 mmol). After 2h, the reaction mixture was concentrated. The residue was recrystalized from MeOH to provide **3** (91 mg, 0.41 mmol, 33% yield) as a white solid. ^{1}H NMR (500 MHz, DMSO-d_6) δ 10.57 (brs, 1H), 7.63 (s, 1H), 6.45 (brs, 2H), 5.07 (s, 1H), 5.05 (t, J = 5.4 Hz, 1H), 4.56 (s, 3H), 3.91(d, J = 5.7 Hz, 2H); ^{13}C NMR (126 MHz, DMSO-d_6) δ 157.01, 153.78, 151.51, 145.86, 137.82, 116.53, 110.25, 62.19, 44.44; MS (ESI) m/z $(M+Na)^+$ calcd.

244.0810, found 244.0827.

Synthesis of L-ala-P-MEP-G (5)

To a solution of **4** (100 mg, 0.452 mmol) in pyridine (15 mL) was added a solution of methylchlorophenylphosphoryl *P*→*N*-L-alaninate in THF (0.2M, 11.3 ml, 2.26 mmol). After addition of *N*-methylimidazole (0.36 mL, 4.52 mmol), the mixture was stired for 16 h. The solvents were evaporated and the residue was re-dissolved into AcOH (6 mL) and stirred at room temperature for overnight. The solution was evaporated, and the residue was purified by silica gel column chromatography (EtOAc-MeOH 9:1 to 7:3, v/v) to provide **5** (33 mg, 0.072 mmol, 16%). ^{1}H NMR (DMSO-d_6, 500 MHz) δ 10.62 (brs, 1H), 7.63 and 7.61 (2s, 1H), 7.41-7.35 (m, 2H), 7.22-7.16 (m, 3H), 6.48 (brs, 2H), 6.16-6.05 (m, 1H), 5.22 and 5.18 (2s, 1H), 4.70 (s, 1H), 4.61 and 4.58 (2s, 2H), 4.54 (d, J = 6.3 Hz, 2H) and 4.49 (*d*, J = 5.7 Hz, 2H), 3.91-3.81 (m, 1H), 3.61 and 3.59 (2s, 3H), 1.26-1.19 (m, 3H); ^{13}C NMR (DMSO-d_6, 126 MHz) δ 173.98 and 173.90 (2d, J = 4.8 Hz), 157.06, 153.91, 151.56, 150.86 and 150.83, 140.63 and 140.53, 137.76, 129.91, 124.90, 120.50 and 120.47, 116.61, 114.00 and 113.74, 66.56 and 66.40 (2d, J = 4.8 Hz), 52.16, 50.03 and 49.90, 44.12 and 44.07, 19.87; MS (ESI) m/z $(M+H)^+$ calcd. 463.1495; found 463.1540.

2-Acetylamino-9-[4-(*tert*-butyldiphenylsilyloxy)-2-methylenebutyl]-9*H*-purin-6-yl diphenylcarbamate (17)

To a solution of **16** (1.50 g, 4.40 mmol), triphenylphosphine (1.38 g, 5.28mmol) and **11** (2.05 g, 5.28mmol) in THF (35 mL) was added DIAD (1.07 g, 5.28 mmol) in THF (7 mL). The reaction mixture was heated to 70 °C and stirred for 2 h. After cooling, the mixture was filtered through a celite pad. The filtrate was evaporated, and the residue was purified by silica gel column chromatography (Hexane-EtOAc 6:4 to 3:7, v/v) to provide compound **17** (2.17 g, 3.05 mmol, 69% yield) as a white foam. ^{1}H NMR ($CDCl_3$, 500 MHz) δ 7.92 (brs, 1H), 7.82 (s, 1H), 7.65-7.62 (m, 4H), 7.47-7.34 (m, 16H), 5.04 (s, 1H), 4.84 (s, 1H), 4.70 (s, 2H), 3.80 (t, J = 6.3 Hz, 2H), 2.50 (s, 3H), 2.24 (t, J = 6.3 Hz, 2H), 1.05 (s, 9H) ; ^{13}C NMR ($CDCl_3$, 126MHz) δ 171.11, 156.12, 155.10, 152.16, 150.38, 143.98, 141.72, 140.85, 135.49, 133.31, 129.82, 129.17, 127.73, 125.92, 120.48, 115.42, 62.58, 48.48, 36.48, 26.82, 25.12, 19.14; MS (ESI) m/z $(M+Na)^+$ calcd. 733.2935; found 733.2924.

2-Amino-9-[4-((*tert*-butyldiphenylsilyloxy)-2-methylenebutyl)-1*H*-purin-6(9*H*)-one (18)

A solution of compound **17** (1.00 g, 1.41 mmol) in 2M NH_3 (MeOH sol) (8 mL) was stirred at 70 °C for 2h. The solution was evaporated, and the residue was

purified by silica gel column chromatography (CH_2Cl_2-MeOH 97:3 to 94:6, v/v) to provide **18** (540 mg, 1.14 mmol, 81% yield) as a white foam. ^{1}H NMR (DMSO-d_6, 500 MHz) δ 10.56 (brs, 1H), 7.64-7.58 (m, 4H), 7.54 (s, 1H), 7.50-7.41 (m, 6H), 6.39 (brs, 2H), 4.90 (s, 1H), 4.60 (s, 1H), 4.50 (s, 2H), 3.74 (t, J = 6.7 Hz, 2H), 2.26 (t, J = 6.7 Hz, 2H), 0.98 (s, 9H) ; ^{13}C NMR (DMSO-d_6, 126 MHz) δ 157.01, 153.78, 151.46, 142.15, 137.58, 135.22, 133.25, 130.08, 128.12, 116.56, 113.03, 63.23, 47.08, 36.51, 26.84, 18.94; MS (ESI) m/z $(M+Na)^+$ calcd. 496.2145; found 496.2187.

2-Amino-9-(4-hydroxy-2-methylenebutyl)-1*H*-purin-6(9*H*)-one (6)

To a solution of **18** (437 mg, 0.923 mmol) in THF (35 mL) was added 1M TBAF in THF (1.11 ml, 1.11mmol). The mixture was stirred at room temperature for 1 h. The solvent was removed, and the residue was purified by silica gel column chromatography (CH_2Cl_2-MeOH 9:1 to 2:8, v/v) to provide **6** (130 mg, 0.55 mmol, 60% yield) as a white foam. ^{1}H NMR (DMSO-d_6, 500 MHz) δ 10.58 (brs, 1H), 7.61 (s, 1H), 6.45 (brs, 2H), 4.88 (s, 1H), 4.60 (t, J = 5.2 Hz, 1H), 4.53 (s, 2H), 4.50 (s, 1H), 3.52 (dt, J = 6.8, 5.2 Hz, 2H), 2.14 (t, J = 6.8 Hz, 2H); ^{13}C NMR (DMSO-d_6, 125 MHz) δ 157.08, 153.82, 151.54, 143.07, 137.85, 116.51, 111.97, 59.64, 47.15, 36.99; MS (ESI) m/z $(M+Na)^+$ calcd. 258.0967; found 258.0966.

Synthesis of L-ala-P-MEB-G (7)

To a solution of **6** (50 mg, 0.213 mmol) in pyridine (7.5 mL) was added a solution of methyl chlorophenylphosphoryl *P*→*N*-L-alaninate in THF (0.2M, 5.3 ml, 1.06 mmol). After addition of *N*-methylimidazole (0.17 mL, 2.13 mmol), the mixture was stirred for 16 h. The solvents were evaporated and the residue was re-dissolved into AcOH (6 mL) and stirred at room temperature for overnight. The solution was evaporated, and the residue was purified by silica gel column chromatography (CH_2Cl_2-MeOH 97:3 to 91:9, v/v) to provide **7** (58 mg, 0.12 mmol, 57%).^{1}H NMR (DMSO-d_6, 500 MHz) δ 10.59 (brs, 1H), 7.61 and 7.59 (2s, 1H), 7.44-7.28 (m, 2H), 7.25-7.08 (m, 3H), 6.45 (s, 2H), 6.09-5.91 (m, 1H), 4.95 and 4.93 (2s, 1H), 4.58 and 4.57 (2s, 1H), 4.55 and 4.53 (2s, 2H), 4.21-4.07 (m, 2H), 3.89-3.79 (m, 1H), 3.59 and 3.58 (2s, 3H), 2.39-2.30 (m, 2H), 1.26-1.18 (m, 3H) ; ^{13}C NMR (DMSO-d_6, 126 MHz) δ 174.02 and 173.90 (2d, J = 4.8 Hz), 157.06, 153.85, 151.55, 150.94, 141.38 and 141.30, 137.77, 129.82, 124.74, 120.41, 116.54, 113.07 and 113.01, 64.29 and 64.23 (2d, J = 4.8 Hz), 52.10, 50.04 and 49.87, 46.82 and 46.80, 34.02 and 33.98, 19.88; MS (ESI) m/z $(M+H)^+$ calcd. 477.1651; found 477.1700.

2-Acetylamino-9-[(diisopropoxyphosphorylmethoxy)allyl]-6-diphenylcarbamoyl

purine (20)

To a solution of (2-hydroxymethylallyloxymethyl)phosphonic acid diisopropyl ester **19** (2.13 g, 8.00 mmol), triphenylphosphine (2.73 g, 10.4 mmol) and **11** (3.73 g, 9.60mmol) in THF (40 mL) was added DIAD (1.94 g, 9.60 mmol). The reaction mixture was heated to 70 °C and stirred for 2 hr. After cooling, the mixture was filtered through a celite pad. The filtrate was evaporated, and the residue was purified by silica gel column chromatography (EtOAc-MeOH 100:0 to 92:8, v/v) to provide **20** (3.14 g, 4.93 mmol, 62% yield) as a pale yellow foam. ^{1}H NMR (500 MHz, CD_3OD) δ 8.31 (s, 1H), 7.49-7.27 (m, 10H), 5.31 (s, 1H), 5.10 (s, 1H), 4.97 (s, 2H), 4.79-4.65 (m, 2H), 4.10 (s, 2H), 3.74 (d, J = 8.6 Hz, 2H), 2.31 (s, 3H), 1.36 (dd, J = 8.0, 6.3 Hz, 12H); ^{13}C NMR (126 MHz, CD_3OD) δ 172.63, 157.21, 156.76, 154.14, 152.58, 147.49, 143.55, 141.76, 130.61, 128.61, 121.78, 117.98, 72.24 (d, J = 12.0 Hz), 73.46 (d, J=6.0 Hz), 65.53 (d, J=167.9 Hz), 47.06, 25.06 , 24.62 (d, J = 3.6 Hz), 24.58 (d, J = 4.8 Hz); MS (ESI) m/z $(M+H)^+$ calcd. 637.2540, found 637.2569.

9-[(diisopropoxyphosphorylmethoxy)allyl]guanine (21)

Compound **20** (361 mg, 0.567 mmol) was dissolved in ca. 9 M ammonia in methanol (5 mL) and heated to 70 °C in sealed tube. After 2h, the reaction mixture

was concentrated and purified by silica gel column chromatography (CH_2Cl_2-MeOH 95:5 to 88:12, v/v) to provide **21** (123 mg, 54% yield) as a white solid. ^{1}H NMR (500 MHz, $CDCl_3$) δ 11.81 (brs, 1H), 7.60 (s, 1H), 7.00 (brs, 2H), 5.22 (s, 1H), 4.86-4.79 (m, 3H), 4.62 (s, 2H), 4.12 (s, 2H), 3.78 (d, J = 9.7 Hz, 2H), 1.36 (dd, J = 8.0 and 6.3 Hz, 12H); ^{13}C NMR (126 MHz, $CDCl_3$) δ 158.40, 154.49, 151.16, 139.67, 137.52, 117.12, 116.53, 74.41 (d, J = 14.4 Hz), 71.85 (d, J = 6.0 Hz), 64.78 (d, J = 171.5 Hz), 44.69, 24.07 (d, J = 3.6 Hz), 24.03(d. J = 4.8 Hz); MS (ESI) m/z $(M+Na)^+$ calcd. 422.1569, found 422.1581.

9-[2-(Hydroxymethyl)allyloxymethylphosphonic acid]guanine (22)

To a solution of **21** (475 mg, 1.19 mmol) in CH_2Cl_2 (10 mL) was added TMSBr (910 mg, 5.95 mmol). The reaction mixture was stirred at room temperature for overnight. The reaction mixture was diluted with CH_2Cl_2 and extracted with water. The aqueous layer was lyophilized and the residue was purified by ODS column chromatography (H_2O-MeOH 95:5 to 7:3, v/v) to provide **22** (278 mg, 74% yield) as a white solid. ^{1}H NMR (500 MHz, D_2O) δ 8.72 (s, 1H), 5.38 (s, 1H), 5.11 (s, 1H), 4.88 (s, 2H), 4.10 (s, 2H), 3.58 (d, J = 9.2 Hz, 2H); ^{13}C NMR (126 MHz, D_2O) δ 158.52, 157.93, 152.92, 141.08, 140.82, 121.33, 111.85, 76.00 (d, J = 13.2 Hz), 68.34 (d, J = 158.4 Hz), 49.37; MS (ESI) m/z $(M-H)^-$ calcd. 314.0654 found

314.0690.

9-[Bis-*O*-(pivaloyoxymethyl)phosphorylmethoxy]allyl]guanine (8)

To a solution of **22** (101 mg, 0.320 mmol), triethylamine (179 μL, 1.28 mmol) and tetrabutylammonium bromide (103 mg, 0.320 mmol) in *N*-methylpyrrolidone (3 mL) was added chloromethyl pivalate (241 mg, 1.60 mmol). The reaction mixture was heated to 50 °C and stirred for 20 hr. The reaction was quenched with MeOH and directly applied to silica gel column chromatography (CH_2Cl_2-MeOH 98:2 to 9:1, v/v). Appropriate fractions were evaporated, triturated from acetonitrile/water=1/1 to provide **8** (17.0 mg, 10% yield) as a white solid. ^{1}H NMR (500 MHz, CD_3OD) δ 7.72 (s, 1H), 5.74-5.69 (m, 4H), 5.26 (s, 1H), 4.94 (s, 1H), 4.71 (s, 2H), 4.11 (s, 2H), 3.93 (d, J = 8.6 Hz, 2H), 1.22 (s, 18H); ^{13}C NMR (126 MHz, CD_3OD) δ 178.42, 159.69, 155.64, 153.53, 142.19, 140.25, 117.75, 117.37, 83.52 (d, J = 6.0 Hz), 75.22 (d, J = 14.4 Hz), 64.81 (d, J = 166.74 Hz), 46.04, 40.03, 27.51; MS (ESI) m/z $(M+Na)^+$ calcd. 566.1992 found 566.1963.

Cell culture, anti-HBV assay and cytotoxicity assay

HepG2 2.2.15 human hepatoblastoma cell line, which can stably produce HBV particles,[11] was kindly gifted from B. Korba of Georgetown University. The HepG2 2.2.15 cells were cultured in Dulbecco's modified Eagle's medium (DMEM; Gibco,

USA) and MT-4 cells were grown in RPMI 1640-based culture medium, which supplemented with 10% (v/v) fetal calf serum (FCS; Gibco, USA) and 50 U/ml penicillin and 50 μg/ml streptomycin.

The HepG2 2.2.15 cells were plated at 1 x 10^5/mL in the presence or absence of various concentrations of a test compound in 96-well microtiter culture plates, then followed by incubation at 37 °C for 6 days. After incubation, the concentration of HBV DNA in the supernatant was determined.

Cytotoxicity of a compound in MT-4 cells was also determined. Cells were plated in a 96-well plate at a density of 1 × 10^5/mL and cultured in the absence or the presence of various concentrations of a compound at 37°C for 7 days. After 100 ml of the medium was removed from each well, 10 ml of 3-(4,5-dimetylthiazol-2-yl)-2,5-diphenyltetrazolium bromide (MTT) solution (Nacalai Tesque, Kyoto, Japan) was added to each well in the plate, followed by incubation at 37 °C for 2 h. After incubation to dissolve the formazan crystals, 100 ml of acidified isopropanol containing 4% (v/v) Triton X-100 was added to each well, and the optical density was measured in a kinetic microplate reader (Vmax; Molecular Devices, Sunnyvale, CA).

Detection of HBV DNA by real-time quantitative polymerase chain reaction

Viral DNA in the supernatants was extracted using QIAamp MinElute Virus Spin Kit (Qiagen, Valencia, CA) according to the manufacture's instruction. HBV DNA was quantified by real-time PCR relative to an external plasmid DNA standard on a Light Cycler instrument using LightCycler® FastStart DNA Master^{PLUS} SYBR Green I

(Roche, Mannheim, Germany) and primers HBV-RT-F (5′-GAGTCTAGACTCGTGGTGGA-3′) and HBV-RT-R (5′-TGAGGCATAGCAGCAGGATG- 3′), which amplified a 184-bp fragment in the RT region of the HBV genome. The PCR conditions used were an initial 3 min at 95 °C, followed by 40 cycles of 95 °C for 10 s, 55 °C for 10 s, and 72 °C for 10 s.

Acknowledgement

Financial supports from Japan Society for the Promotion of Science (KAKENHI No. 24590144 to K. H.) and a Health and Labor Sciences Research Grant [Practical Research on Hepatitis (Research on the innovative development and the practical application of new drugs for hepatitis B)] are gratefully acknowledged.

References

(1) White, D. O.; Fenner, F. J. *Medical Virology*, *4th ed*; Academic: New York, 1994; Chapter 22.

(2) Dienstag, J. L. Drug therapy: hepatitis B virus infection. *N. Engl. J. Med.* **2008**, *359*, 1486-1500.

(3) (a) Innaimo, S. F.; Seifer, M.; Bisacchi, G. S.; Stabdring, D. N.; Zahler, R.; Colonno, R. J. Identification of BMS-200475 as a potent and selective inhibitor of hepatitis B virus. *Antimicrob. Agents Chemother.* **1997**, *41*, 1444-1448. (b) Yamanaka, G.; Wilson, T.; Innaimo, S.; Bisacchi, G. S.; Egli, P.; Rinehart, J. K.; Zahler, R.; Colonno, R. J. Metabolic studies on BMS-200475, a new antiviral compound active against hepatitis B

virus. *Antimicrob. Agents Chemother.* **1999**, *43*, 190-193.

(4) De Clercq, E. Ten paths to the discovery of active nucleoside and nucleotide analogues. *Nucleosides, Nucleotides and Nucleic Acids*, **2012**, *31*, 339-352 and references cited therein.

(5) (a) Will, H.; Reiser, W.; Weimer, T.; Pfaff, E.; Büscher, M.; Sprengel, R.; Cattaneo, R.; Schaller, H. Replication strategy of human hepatitis B virus. *J. Virol.* **1987**, *61*, 904-911. (b) Scott, L. J.; Kieting, G. M. Entecavir. *Drugs*, **2009**, *69*, 1003-1033.

(6) Kim, A.; Hong, H. Synthesis and antiviral evaluation of novel exomethylene acyclic nucleosides and phosphonic acid nucleosides. *Arch. Pharm. Chem. Life Sci*, **2005**, *338*, 528-533.

(7) Zou, R.; Robins, M. J. High-yield regioselective synthesis of 9-glycosyl guanine nucleosides and analogues via coupling with 2-*N*-acetyl-6-*O*-diphenylcarbamoylguanine. *Can. J. Chem.* **1987**, *65*, 1436-1437.

(8) Qiu, Y.-L.; Ptak, R. G.; Breitenbach, J. M.; Lin, J.-S.; Cheng, Y.-C.; Drach, J. C.; Kern, E. R.; Zemlicka, Synthesis and antiviral activity of phosphoralaninate derivatives of methylenecyclopropane analogs of nucleosides. *Antiviral Research*, **1999**, 43, 37-53.

(9) Weigant, S.; Brückner, R. Direct preparation of allylstannanes from allyl alcohols: convenient synthesis of β-substituted allylstannanes and of stereodefined δ-substituted allylstannanes. *Synthesis*, **1996**, 475-482

(10) (a) Choi, J.-R.; Cho, D.-G; Roh, K. Y.; Hwang, J.-T.; Ahn, S.; Jang, H. S.; Cho, W.-Y.; Kim, K. W.; Cho, Y.-G.; Kim, J.; Kim, Y.-Z. A novel class of phosphonate nucleosides. 9-[(1-phosphonomethoxycyclopropyl)methyl]guanine as a potent and selective anti-HBV agent. *J. Med. Chem.* **2004**, *47*, 2864-2869. (b) Roux, L.; Priet, S.; Payrot, N.; Weck, C.; Fournier, M.; Zoulim, F.; Balzarini, J.; Canard, B.; Alvarez, K.

Ester prodrugs of acyclic nucleoside thiophosphonates compared to phosphonates: synthesis, antiviral activity and decomposition study. *Euro J. Med. Chem.* **2013**, *63*, 866-881.

(11) Sells, M. A.; Chen, M. L.; Acs, G. Production of hepatitis B virus particles in Hep G2 cells transfected with cloned hepatitis B virus DNA, *PNAS* **1987**, *84*, 1005-1009.

Journal of Infectious Diseases Advance Access published March 31, 2014

MAJOR ARTICLE

Effect of Hepatitis B Virus Reverse Transcriptase Variations on Entecavir Treatment Response

Danny Ka-Ho Wong,[1,2] Malgorzata Kopaniszen,[1] Katsumi Omagari,[4] Yasuhito Tanaka,[4] Daniel Yee-Tak Fong,[3] Wai-Kay Seto,[1] James Fung,[1,2] Fung-Yu Huang,[1] An-ye Zhang,[1] Ivan Fan-Ngai Hung,[1] Ching-Lung Lai,[1,2] and Man-Fung Yuen[1,2]

[1]Department of Medicine, [2]State Key Laboratory for Liver Research, and [3]School of Nursing, University of Hong Kong, Hong Kong SAR; and [4]Department of Virology and Liver Unit, Nagoya City University Graduate School of Medical Sciences, Japan

Background. Entecavir therapy often reduces hepatitis B virus (HBV) DNA to an undetectable level, but HBV DNA remain detectable in some patients. We investigated whether baseline HBV reverse transcriptase (rt) polymorphism and quasispecies complexity and diversity were associated with treatment response.

Methods. Pretreatment HBV DNA levels, HBV rt sequence, serology, and quasispecies complexity and diversity from 305 entecavir-treated patients were determined. These data were tested for their association with year 1 virological outcome, defined by optimal response (undetectable HBV DNA; lower limit of detection, ≤12 IU/mL) or partial response (detectable HBV DNA).

Results. Four rt variants were more frequently detected in the 64 partial responders than in the 241 optimal responders (all $P < .05$). Multivariate analysis revealed that high baseline HBV DNA level ($P < .0001$; odds ratio [OR], 2.32), HBV e antigen (HBeAg) positivity ($P < .001$; OR, 3.70), and rt124N ($P = .002$; OR, 3.06) were associated with a partial entecavir response. Compared with the optimal responders, the partial responders had a lower quasispecies complexity and diversity.

Conclusions. Apart from the known factors (high baseline HBV DNA level and HBeAg positivity), a novel single nucleotide polymorphism (rt124N) and lower quasispecies complexity and diversity were associated with partial entecavir response at year 1.

Keywords. antiviral therapy; hepatitis B; chronic viral hepatitis; drug response.

Nucleos(t)ide analogue (NA) therapy is currently the mainstay of treatment for chronic hepatitis B virus (HBV) infection worldwide. One of the problems of administering NAs for the treatment of chronic HBV infection is the development of drug-resistant mutations after prolonged treatment. Although the incidence of resistance to the current 2 first-line NAs, entecavir and tenofovir, is low, there are situations, such as severe acute exacerbation of chronic hepatitis B, in which more-rapid lowering of the HBV DNA level is preferred. Moreover, it has been found that early viral suppression to an undetectable level during the first year of therapy is important in reducing the chance of development of drug resistance [1–4].

According to 2 multicenter pivotal phase III entecavir clinical trials [5, 6], around 10%–35% of patients receiving entecavir still have detectable HBV DNA after 1 year of treatment. A rational hypothesis is that there may be some differences within the natural polymorphism in the HBV "wild-type" reverse transcriptase (rt) sequences that confer primary hypo-responsiveness. This approach has been used to predict antiviral response in human immunodeficiency virus (HIV)–infected patients [7].

So far, only a limited number of small cohort or case report studies have investigated the association between pretreatment HBV rt natural variants and NA treatment response [8–16]. Large-scale studies with statistically significant findings are lacking, and studies

Received 12 December 2013; accepted 27 February 2014.

Presented in part: International Liver Congress, Amsterdam, the Netherlands, 24–28 April 2013. Abstract 779.

Correspondence: Man-Fung Yuen, MD, PhD, Department of Medicine, The University of Hong Kong, Queen Mary Hospital, Pokfulam Rd, Hong Kong, China (mfyuen@hku.hk).

The Journal of Infectious Diseases

© The Author 2014. Published by Oxford University Press on behalf of the Infectious Diseases Society of America. All rights reserved. For Permissions, please e-mail: journals.permissions@oup.com.

DOI: 10.1093/infdis/jiu133

on the predictive HBV rt sequences for entecavir treatment are scarce.

In this study, our primary aim was to investigate whether there are some pretreatment HBV rt sequence variations that can predict response to entecavir. Identifiable sequence variations would be subjected to a molecular docking stimulation analysis to determine the possible underlying mechanisms [17]. It is not known whether viral quasispecies heterogeneity will affect entecavir response. The secondary aim was to examine whether there was an association between baseline quasispecies complexity and diversity with response to entecavir.

METHODS

Study Subjects

We recruited 370 patients with chronic hepatitis B who started entecavir therapy between January 2002 and September 2009 in the Liver Clinic at the Queen Mary Hospital, Hong Kong. None of these 370 patients had received prior NA therapy or interferon/pegylated-interferon therapy or had other chronic liver diseases, including chronic hepatitis C virus and hepatitis D virus coinfection, autoimmune diseases, and alcoholic liver diseases. All 370 patients had taken 0.5 mg of entecavir continuously, had been followed-up in our clinic for >1 year, and had baseline, year 1, and year 3 (if applicable) HBV DNA levels measured. Liver cirrhosis was defined by the presence of cirrhosis-related complications, such as ascites, and esophageal/gastric varices, with or without ultrasonographic evidence of small-sized or nodular-surfaced liver. All patients consented to have baseline and subsequent serum samples stored for analysis. This study was approved by the Institutional Review Board of The University of Hong Kong and Hospital Authority Hong Kong West Cluster, Hong Kong.

HBV DNA Levels and Definition of Treatment Response

HBV DNA levels were measured by the Cobas TaqMan HBV Test (Roche Diagnostics, Branchburg, NJ), which has a lower limit of detection of 12 IU/mL (60 copies/mL) and a linear range of up to 1.1×10^8 IU/mL (6.4×10^8 copies/mL). For statistical and numerical analysis, samples with a viral load of $>1.1 \times 10^8$ IU/mL were regarded to have a viral load of 1.1×10^8 IU/mL. Optimal and partial virological responses were defined as undetectable HBV DNA by the Cobas TaqMan assay ($\leq$12 IU/mL) and detectable HBV DNA (>12 IU/mL), respectively, at the end of 1 year of treatment [18].

Direct Polymerase Chain Reaction (PCR) Sequencing of the Gene Encoding HBV rt

HBV DNA was isolated from 200 μL of serum samples, using the QIAamp DNA blood mini kit (Qiagen, Hilden, Germany). The HBV polymerase rt domain was PCR amplified using the Platinum Taq High Fidelity DNA Polymerase, the forward primer HBV56s (5′-CCTGCTGGTGGCTCCAGTTC-3′), and the reverse primer HBV1234a (5′-GACACAAAGGTCCCACG-CAT-3′). The 1.1-kb amplicon was sequenced bidirectionally, using the BigDye Terminator v3.1 Cycle Sequencing Kit and the Applied Biosystems Prism 3730*xl* Genetic Analyzer (Life Technologies, Carlsbad, CA).

Clonal Sequencing

PCR amplicons were cloned into the TA cloning sequencing vector system (Life Technologies) and transformed into competent *Escherichia coli* JM109 cells. For each isolate, 10–20 white colonies (median, 18 colonies) were picked and sequenced, as described above.

DNA Sequence Analysis

HBV DNA sequences were assembled and aligned using the CLC Main Workbench 6.6.2 (CLC Bio, Katrinebjerg, Denmark). HBV quasispecies heterogeneity was evaluated by 2 parameters: quasispecies complexity and quasispecies diversity. Quasispecies complexity is a measure of heterogeneity within a sample, while quasispecies diversity refers to the relatedness (genetic distance) of individual genomes within the population. Complexity is measured by normalized Shannon entropy (Sn) at both nucleotide and amino acid levels, using the following formula: $Sn = -\Sigma_i [p_i \times \ln p_i]/\ln N$, where p_i is the observed proportion of each different sequence of the mutant spectrum, and N the total number of clones compared [19]. Normalized Sn ranges from 0 (when all clones are conserved) to 1 (when all clones are different). Quasispecies diversity was assessed by the mean genetic distance (d) at both nucleotide and amino acid levels, the number of synonymous substitutions per synonymous site (dS), and the number of nonsynonymous substitutions per nonsynonymous site (dN), using the MEGA software [20, 21].

Molecular Docking Simulation

As there are no data on the crystal structures of the HBV rt, the crystal structures of the HIV type 1 (HIV-1) rt heterodimer (Protein Data Bank accession number 3KLI) were used as a template for molecular modeling [22]. Protein-compound docking simulation was performed by the Sievegene module in the myPresto Program and an in-house program OPPIH (Option Program for myPresto In HTML tools) [23, 24].

Statistical Analysis

Statistical analyses were performed using SPSS 18.0 (SPSS, Chicago, IL). Continuous variables with normal and skewed distributions were compared using the Student t test and the Mann-Whitney test, respectively. Categorical variables were tested using the χ^2 test or the Fisher exact test as appropriate. Bonferroni correction was used to control for type I error in multiple comparisons. Stepwise logistic regression was performed to test the factors associated with complete or

Downloaded from http://jid.oxfordjournals.org/ at Bristol-Myers Squibb on May 9, 2014

partial virological response. Statistical significance was denoted by $P < .05$.

RESULTS

Baseline Characteristics

Full-length HBV rt DNA was successfully amplified by PCR in 305 patients. Of these 305 patients, 114 (37%) were HBV e antigen (HBeAg) positive and 191 (63%) were HBeAg negative at baseline. At baseline, 87 patients (29%) had clinical evidence of liver cirrhosis. At year 1, 64 patients (21%) had partial virological response to entecavir (HBV DNA level, >2 IU/mL). The median HBV DNA level at year 1 for the partial responders was 110 IU/mL (range, 12.4×10^6 –5.12×10^6 IU/mL). The baseline characteristics of the 305 patients are listed in Table 1. The sex ratios, baseline albumin levels, and bilirubin levels were comparable between the partial and optimal responders. Compared with the optimal responders, the partial responders were younger, had greater proportions of HBeAg-positive patients, and had higher baseline HBV DNA and alanine aminotransferase (ALT) levels. Compared with the optimal responders, the partial responders also had a greater proportion of patients with HBV genotype B and a smaller proportion of patients with cirrhosis.

HBV rt Sequence Analysis

The amino acid sequence for the whole HBV rt region (344 amino acids) was studied. Major known drug resistance mutations (rtL80I/V, I169T, V173L, L180M, A181V/T, T184G, A194T, S202I, M204I/V, N236T, and M250V) were not detected in these patients, except that, in one patient, concomitant rtL80I and rtL180M mutations were detected. Of the 344 rt amino acid positions, 217 amino acid residues were conserved among these 305 patients. Twenty rt variations were found only in partial responders (distributed among 17 partial responders) but not in any of the optimal responders (Supplementary Table 1). Because of the rarity of these cases, association between these polymorphisms and partial/slow response was not statistically different.

Association analysis revealed that 17 amino acid variants were detected more frequently in the 64 partial responders than in the 241 optimal responders (Table 2). Since multiple comparisons of 127 nonconserved amino acid positions were performed, Bonferroni correction was used to control for type I error. After Bonferroni adjustment, 4 rt variants, namely rt53N, rt118N, rt124N, and rt332S, occurred significantly more frequently in the partial responders than in the optimal responders (Table 2). Of these 305 patients, 52 harbored HBV with all 4 variants (rt53N, rt118N, rt124N, and rt332S). The proportion of patients harboring all of these 4 variants was higher in the partial responders (25/64 [39%]) than in the optimal responders (27/241 [11%]; $P < .0001$).

We investigated the HBV rt sequence at year 1 in the partial responders. We successfully amplified the HBV rt region in 18 partial responders, all with an HBV DNA level of >500 IU/mL at year 1. HBV entecavir resistance mutations were not detected.

Table 1. Baseline Characteristics of Patients With an Optimal or Partial Response to Entecavir

Characteristic	Optimal Responders (n = 241)	Partial Responders (n = 64)	*P*
Age, y, mean ± SD	48.3 ± 13.1	41.5 ± 10.7	<.001
Sex, male:female	167:74	42:22	.574
HBeAg positivity, patients, no. (%)	67 (28)	47 (73)	<.001
HBV DNA level, $\log_{10}$ IU/mL	6.2 (2.3–8.0)	8.0 (4.4–8.0)	<.001
HBV genotype, B:C	65:176	30:33[a]	.002
Cirrhosis, patients, no. (%)	78 (32)	9 (14)	.004
ALT level, U/L	77 (11–3000)	110 (20–2144)	.004
Albumin level, g/L	42 (22–51)	42 (25–48)	.459
Total bilirubin level, μmol/L	12 (4–261)	13 (2–216)	.256

Continuous parameters are expressed as median value (range), unless otherwise indicated.

Abbreviations: ALT, alanine aminotransferase; HBeAg, hepatitis B virus e antigen; HBV, hepatitis B virus.

[a] One patient had HBV genotype A.

Table 2. Reverse Transcriptase (rt) Variants With Significantly Different Distribution Among Patients With an Optimal or Partial Response to Entecavir

rt Variant	Percentage of Variants Found in Partial Responders	Percentage of Variants Found in Optimal Responders	*P*	
			Unadjusted	After Bonferroni Correction
rt9H	68.8	53.0	.025	1
rt16T	50.0	29.6	.002	.254
rt53N	51.6	27.4	.00024	**.031**
rt109S	54.7	35.3	.005	.635
rt118N	48.4	25.3	.00034	**.043**
rt121I	51.6	29.5	.001	.127
rt124N	50.0	23.7	.000038	**.0048**
rt127R	46.9	29.0	.007	.889
rt131N	50.0	28.2	.001	.127
rt134N	35.9	16.2	.00048	.061
rt151Y	51.6	30.3	.001	.127
rt221Y	53.1	37.8	.026	1
rt222A	40.6	21.6	.002	.254
rt238H	50.0	31.1	.005	.635
rt271M	48.4	26.1	.001	.127
rt278V	70.3	54.8	.025	1
rt332S	43.8	20.1	.00010	**.013**

rt variants with significant different distribution after Bonferroni correction are shown in bold.

Compared with baseline, no change in the variants at year 1 at positions rt53, rt118, rt124, and rt332 was observed, indicating that these variants persisted over time in these patients.

The relationship between these 4 rt variants and other baseline parameters were studied. The 4 rt variants were distributed equally in patients of different sexes and HBeAg statuses (all $P > .05$). However, these 4 variants were found more frequently among patients without cirrhosis, those with HBV genotype B, and those with a high HBV DNA level (all $P < .05$).

Multivariable logistic regression analysis was performed to determine the independent effects of the baseline factors of age, HBeAg status, liver cirrhosis, ALT level, HBV DNA level, HBV genotype, and rt variants on partial entecavir response at year 1. We found that high baseline HBV DNA levels ($P < .0001$; odds ratio [OR], 2.32; 95% confidence interval [CI], 1.61–3.36), HBeAg positivity ($P < .001$; OR, 3.70; 95% CI, 1.79–7.65), and rt variant rt124N ($P = .002$; OR, 3.06; 95% CI, 1.53–6.11) were associated with partial entecavir response at year 1.

We also studied whether these HBV variants were associated with suboptimal entecavir response if other cutoff HBV DNA levels were used. Of these 305 patients, 13 (4.3%) had an HBV DNA level of >2000 IU/mL at year 1. A higher proportion of patients with an HBV DNA level of >2000 IU/mL had the rt124N variant, compared with patients with an HBV DNA level of ≤2000 IU/mL (7/13 [53.8%] vs 82/292 [28.1%]; $P = .046$). However, no significant difference in the variant frequencies of rt53N, rt118N, and rt332S was found ($P = .281$, .057, and .076, respectively). When other cutoff HBV DNA levels, such as 1000 IU/mL and 200 IU/mL, were used, no significant differences in the HBV variant frequencies were found (data not shown).

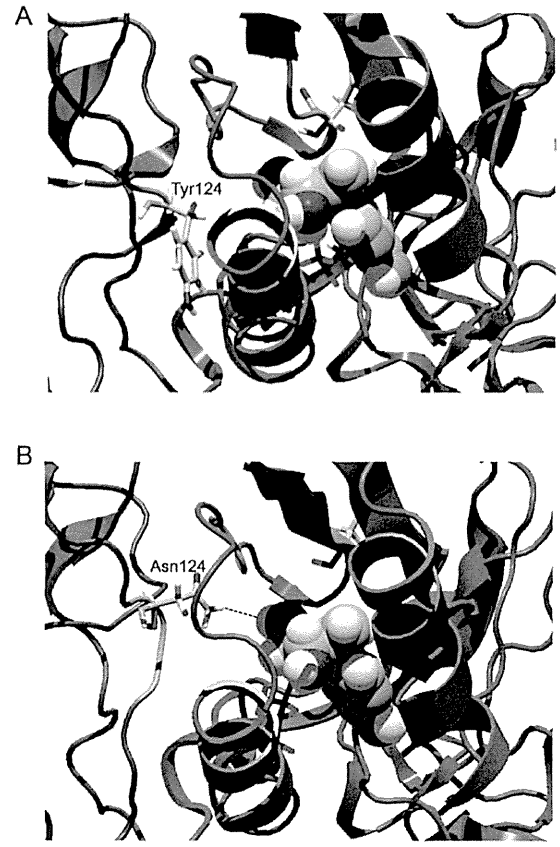

Figure 1. Molecular docking simulation model of the hepatitis B virus (HBV) reverse transcriptase (rt) catalytic domain. The HBV subunits corresponding to the human immunodeficiency virus type 1 rt p66 and p51 subunits are shown as blue and green ribbons, respectively. The entecavir molecule is shown in the middle, with a 3D space-filling representation. The figures were created using MolFeat (FiatLux, Tokyo, Japan). *A*, Catalytic pocket of rt with rt124Y (Tyr124). *B*, Catalytic pocket of rt with rt124N (Asn124).

Molecular Docking Simulation

We used a molecular docking simulation model to assess whether rt124N causes a steric hindrance to the binding of entecavir to HBV rt [17]. On the basis of the crystal structure of the HIV-1 rt, we constructed a molecular model of the catalytic binding pocket of the HBV rt heterodimer (Figure 1). In this model, residue rt124 was positioned behind the helix, which consists of rt180L and rt184T. As shown in Figure 1*A*, rt124Y, the prevailing rt sequence for HBV genotype C, did not interfere with binding of entecavir to the rt catalytic pocket. In contrast, rt124N, the prevailing sequence of HBV genotype B, was in close proximity to entecavir and might cause a slight interference to the binding of entecavir to rt (Figure 1*B*).

HBV Quasispecies Complexity and Diversity

Quasispecies complexity and diversity were compared between the optimal and partial responders. As shown in Table 3, the optimal responders had a significantly higher quasispecies complexity than the partial responders at the nucleotide level ($P = .036$), and the quasispecies complexity at the amino acid level also tended to be higher in the optimal responders ($P = .087$). Similarly, the optimal responders had a greater quasispecies diversity than the partial responders in terms of all 4 parameters (mean genetic distance at both the nucleotide and amino acid levels, number of synonymous substitutions per synonymous site, and number of nonsynonymous substitutions per nonsynonymous site; all $P < .05$; Table 3). In other words, lower baseline quasispecies complexity and diversity were associated with partial response to entecavir at year 1.

Longer-Term Entecavir Treatment Response

We also determined whether pretreatment rt variations were associated with differences in longer term treatment response. Among the 64 suboptimal responders, 55 patients had continuous entecavir treatment with year 3 HBV DNA data available. At year 3, 14 of 55 patients (25%) still had detectable HBV